



**HAL**  
open science

## **Kinetic Alfvén wave explanation of the Hall fields in magnetic reconnection**

Lei Dai, Chi Wang, Yongcun Zhang, Benoit Lavraud, James Burch, Craig Pollock, Roy B. Torbert

► **To cite this version:**

Lei Dai, Chi Wang, Yongcun Zhang, Benoit Lavraud, James Burch, et al.. Kinetic Alfvén wave explanation of the Hall fields in magnetic reconnection. *Geophysical Research Letters*, 2017, 44, pp.634-640. 10.1002/2016GL071044 . insu-03677092

**HAL Id: insu-03677092**

**<https://insu.hal.science/insu-03677092>**

Submitted on 25 May 2022

**HAL** is a multi-disciplinary open access archive for the deposit and dissemination of scientific research documents, whether they are published or not. The documents may come from teaching and research institutions in France or abroad, or from public or private research centers.

L'archive ouverte pluridisciplinaire **HAL**, est destinée au dépôt et à la diffusion de documents scientifiques de niveau recherche, publiés ou non, émanant des établissements d'enseignement et de recherche français ou étrangers, des laboratoires publics ou privés.

Copyright

RESEARCH LETTER

10.1002/2016GL071044

Key Points:

- Hall electric field balanced by ion pressure gradient represents the finite ion gyroradius of kinetic Alfvén waves
- KAW physics predicts a ratio of Hall fields ( $E_n/B_m$ ) on the order of a few Alfvén speed
- New perspective on ion intrusion at magnetopause reconnection

Correspondence to:

L. Dai,  
ldai@spaceweather.ac.cn

Citation:

Dai, L., C. Wang, Y. Zhang, B. Lavraud, J. Burch, C. Pollock, and R. B. Torbert (2017), Kinetic Alfvén wave explanation of the Hall fields in magnetic reconnection, *Geophys. Res. Lett.*, *44*, 634–640, doi:10.1002/2016GL071044.

Received 31 AUG 2016

Accepted 3 DEC 2016

Accepted article online 9 DEC 2016

Published online 25 JAN 2017

## Kinetic Alfvén wave explanation of the Hall fields in magnetic reconnection

Lei Dai<sup>1</sup>, Chi Wang<sup>1</sup>, Yongcun Zhang<sup>1</sup>, Benoit Lavraud<sup>2</sup>, James Burch<sup>3</sup>, Craig Pollock<sup>4</sup>, and Roy B. Torbert<sup>5</sup>

<sup>1</sup> State Key Laboratory of Space Weather, National Space Science Center, Chinese Academy of Sciences, Beijing, China,

<sup>2</sup> Institut de Recherche en Astrophysique et Planétologie, Université de Toulouse, Toulouse, France, <sup>3</sup> Southwest Research Institute, San Antonio, Texas, USA, <sup>4</sup> NASA Goddard Space Flight Center, Greenbelt, Maryland, USA, <sup>5</sup> University of New Hampshire, Durham, New Hampshire, USA

**Abstract** Magnetic reconnection is initiated in a small diffusion region but can drive global-scale dynamics in Earth’s magnetosphere, solar flares, and astrophysical systems. Understanding the processes at work in the diffusion region remains a main challenge in space plasma physics. Recent in situ observations from Magnetospheric Multiscale and Time History of Events and Macroscale Interactions during Substorms reveal that the electric field normal to the reconnection current layer, often called the Hall electric field ( $E_n$ ), is mainly balanced by the ion pressure gradient. Here we present theoretical explanations indicating that this observation fact is a manifestation of kinetic Alfvén waves (KAWs) physics. The ion pressure gradient represents the finite gyroradius effect of KAW, leading to ion intrusion across the magnetic field lines. Electrons stream along the magnetic field lines to track ions, resulting in field-aligned currents and the associated pattern of the out-of-plane Hall magnetic field ( $B_m$ ). The ratio  $\Delta E_n/\Delta B_m$  is on the order of the Alfvén speed, as predicted by the KAW theory. The KAW physics further provides new perspectives on how ion intrusion may trigger electric fields suitable for reconnection to occur.

### 1. Introduction

Understanding the physical processes at work in the magnetic reconnection diffusion region is the prime objective of the Magnetospheric Multiscale (MMS) mission [Burch *et al.*, 2016a]. Launched on 13 March 2015, the MMS spacecraft provides unprecedented high-resolution plasma measurements in space [Torbert *et al.*, 2016; Mauk *et al.*, 2016; Pollock *et al.*, 2016]. By resolving kinetic-scale structures and dynamics in the vicinity of the X line region, MMS has already made breakthrough observations that advanced the understanding of reconnection [Burch *et al.*, 2016b; Burch and Phan, 2016].

One of the new insights from MMS concerns the electric field ( $E_n$ ) normal to the reconnection current layer in the diffusion region. Recent MMS observations [Burch *et al.*, 2016b; Wang *et al.*, 2016] (Y. Zhang *et al.*, private communication, 2016) reveal that this normal electric field is mainly balanced by the ion pressure gradient. The accurate comparison between  $E_n$  and the ion pressure gradient is enabled by the fast measurements of the particles and fields from the four MMS spacecraft. The balance between  $E_n$  and the ion pressure gradient has also been inferred using previous Time History of Events and Macroscale Interactions during Substorms (THEMIS) measurements [Dai *et al.*, 2015].

The normal electric field  $E_n$  in reconnection is generally understood as the Hall electric field at the ion kinetic scale. The rationale behind it is the simplified Ohm’s law at the ion scale  $\mathbf{E} + \mathbf{v}_i \times \mathbf{B} = (1/nq)\mathbf{J} \times \mathbf{B}$ , where the Hall term ( $\mathbf{J} \times \mathbf{B}$ ) may dominate the contribution to the electric field. Mathematically, this equation is equivalent to the electron frozen-in condition ( $\mathbf{E} + \mathbf{v}_e \times \mathbf{B} = 0$ ), because the ion terms  $\mathbf{v}_i \times \mathbf{B}$  from both sides can cancel each other. The Hall electric field is an important feature in the reconnection diffusion region. The presence of the Hall electric field associated with the Hall magnetic field indicates a time-varying electromagnetic structure of the Hall signals.

More insights on the nature of  $E_n$  is possible from the ion momentum equation in a collisionless plasma [Cai *et al.*, 1994; Cai and Lee, 1997; Dai *et al.*, 2015],

$$\mathbf{E} + \mathbf{v}_i \times \mathbf{B} = (1/n_i q_i) \nabla \cdot \mathbf{P}_i + (m_i/q_i) d\mathbf{v}_i/dt, \tag{1}$$

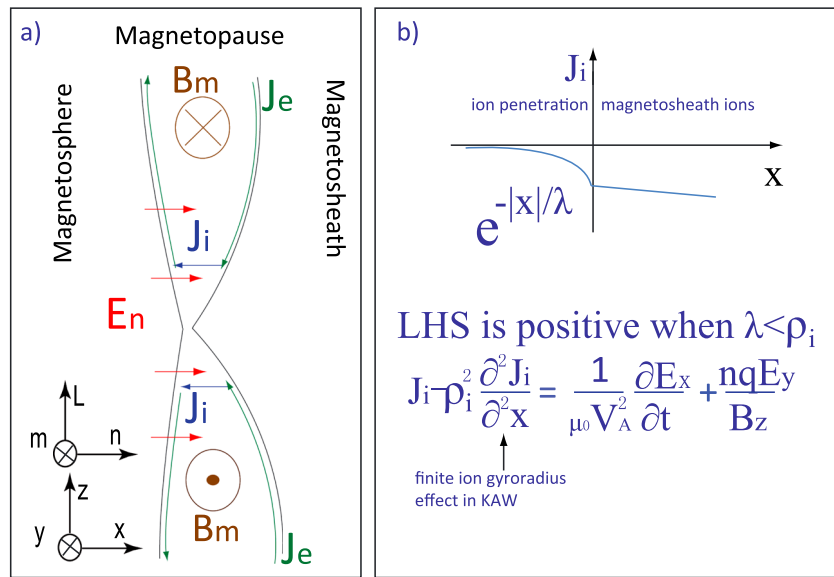


**Figure 1.** Schematics of asymmetric reconnection at the magnetopause. (a) Hall electric field ( $E_n$ ), out-of-plane magnetic field ( $B_m$ ), and Hall current system are explained by KAW physics. (b) Illustration of penetration of ions and various terms of equation (3). See more descriptions in text.

Besides the ion fluid convection term, the inertial term or the pressure gradient can contribute to the electric field. The MMS observation of a normal electric field  $E_n$  mainly balanced by the ion pressure gradient in reconnection has profound implications. In a simple sense, the ion pressure gradient corresponds to the finite gyroradius effect and ion penetration in the reconnection current layer [Burch et al., 2016b; Shay et al., 2016]. In this study, we present a theoretical explanation that the ion pressure gradient represents the finite ion gyroradius effect of kinetic Alfvén waves (KAWs). We will show that the KAW physics also predicts the formation of the electron field-aligned currents, the associated out-of-plane magnetic field ( $B_m$ ), and the ratio  $E_n/B_m$ .

## 2. Normal Electric Fields Induced by Ion Pressure Gradient: Ion Gyroradius Effect in KAW Physics

To show that the balance between  $E_n$  and ion pressure gradient represents the ion gyroradius effect of KAW, we start with the ion momentum (equation (1)) in the direction normal to the reconnection layer. The **LMN** coordinate system for reconnection layer is illustrated in Figure 1. Simply speaking, **L** is along the direction of the magnetic field of the current layer, **M** is the out-of-plane direction, and **N** is outward and normal to the current layer. In the theoretical derivation, we use a **XYZ** coordinate in which **Z** corresponds to **L**, **Y** corresponds to **M**, and **X** corresponds to **N**. The **XYZ** coordinate system is close to the GSM at the subsolar magnetopause.

As indicated by observations [Burch et al., 2016b; Wang et al., 2016; Dai et al., 2015], we can neglect the small ion inertial term  $(m_i/q_i)d\mathbf{v}_i/dt$  in the momentum equation in the normal direction. This approximation is consistent with KAW physics in which the ion inertial term is a small term on the order of  $O(\omega^2/\Omega_i^2)$ , where  $\Omega_i$  is ion gyrofrequency [Cheng and Johnson, 1999; Stasiewicz et al., 2000]. In the normal direction, the main contribution to the pressure gradient is the variation along **N** of the diagonal **NN** component of the pressure tensor in observations. We use an isothermal approximation to rewrite the ion pressure as  $n_i T_i$ , where  $n_i$  is ion number density and  $T_i$  is the ion temperature. The ion  $\mathbf{v}_i \times \mathbf{B}$  term should be small near the stagnation point. But the stagnation point may deviate from the X line. The ion flow could be finite in the diffusion region near the X line [Cassak and Shay, 2007]. Therefore, we keep this term in the derivation. After these simplifications, we have the equation for the Hall electric field

$$\mathbf{E} + \mathbf{v}_i \times \mathbf{B} \approx (1/n_i q_i) \nabla n_i T_i, \quad (2)$$

We want to explore the time-varying aspect of the Hall fields and currents. Motivated by this consideration, we take the partial time derivative of equation (2) in the **X** direction. The result of the first term is  $\partial_t E_x$ . The time derivative of the second term is  $\partial_t V_{iy} B_z$ . We use the approximation  $\delta B_z \ll B_z$ . This is usually adopted

in observations as the current layer changes very little in the timescale of spacecraft crossing. Assuming that  $\partial_y = 0$ , the second term becomes  $(q_i B_z / m_i) E_y - (B_z^2 / n_i m_i) J_{ix} \cdot J_{ix} = n_i q_i V_{ix}$  is the ion current in the normal direction. The time derivative of the pressure gradient term is  $(1/n_i q_i) \nabla \partial_t n_i T_i$ , assuming  $\delta n_i \ll n_i$ . We use charge conservation for the ions  $\partial_t(n_i q_i) + \nabla \cdot \mathbf{J}_i = 0$  to evaluate  $\partial_t n_i$ . The third term becomes  $-(T_i/n_i q_i^2) \partial_{xx} J_{ix}$ . The contribution from ions to the field-aligned current  $J_{iz}$  is a small effect and usually neglected. The field-aligned current is mostly carried by light electrons. In the perpendicular direction, electrons also have an  $\mathbf{E} \times \mathbf{B}$  drift and this will generally cancel the current provided by ion  $\mathbf{E} \times \mathbf{B}$  drift.

Rearranging the terms, we have the following equation describing  $E_n$  and the ion current in the normal direction,

$$J_{ix} - \rho_i^2 \nabla_{xx} J_{ix} = \frac{\partial_t E_x}{\mu_o V_A^2} + \frac{n_i q_i E_y}{B_z} \quad (3)$$

$\rho_i = \sqrt{T_i m_i} / q_i B_z$  is ion thermal gyroradius,  $V_A = \sqrt{(B_z^2 / n_i m_i \mu_o)}$  is the Alfvén speed.

The physical meaning of equation (3) is straightforward. The first term  $\partial_t E_x / \mu_o V_A^2$  on the right-hand side (RHS) is the ion polarization current related to slow time-varying  $E_n$ . The second term  $n_i q_i E_y / B_z$  on the RHS is the  $\mathbf{E} \times \mathbf{B}$  drift caused by the reconnection electric field  $E_y$ . On the left-hand side (LHS), the first term  $J_{ix}$  is the current without corrections from finite ion gyroradius effect. The  $\rho_i^2 \nabla_{xx} J_{ix}$  is the finite gyroradius effect correction. The gyroradius effect results from the ion pressure gradient. Without the finite gyroradius effect,  $J_{ix}$  shall have a one-to-one relation with the local electric fields  $E_x$  and  $E_y$ .

Since its discovery by Hasegawa and Chen [1976], KAWs have been intensively studied in a wide variety of plasmas [Lysak and Lotko, 1996; Wu et al., 1996; Johnson and Cheng, 1997; Streltsov et al., 1998; Stasiewicz et al., 2000; Chaston et al., 2005; Dai, 2009; Keiling, 2009; Shay et al., 2011; Lin et al., 2012; Liang et al., 2016]. In the following, we show that the finite gyroradius effect of KAW represents the ion pressure-based gyroradius effect in equation (3). The perpendicular current of KAWs is provided by ions and related to the electric field as follows [Cheng, 1991; Lysak and Lotko, 1996; Streltsov et al., 1998]:

$$\tilde{J}_{ix} = -i\omega \epsilon_o \frac{c^2}{V_A^2} \frac{1 - e^{-\mu} I_o(\mu)}{\mu} \tilde{E}_x \quad (4)$$

where  $\mu = k_x^2 \rho_i^2$  and  $I_o$  is the modified Bessel function. Following a Pade approximation  $[1 - e^{-\mu} I_o(\mu)] / \mu \approx 1 / (1 + \mu)$  that is good for the arbitrary  $\mu$  [Johnson and Cheng, 1997; Streltsov et al., 1998; Stasiewicz et al., 2000; Lysak, 2008], the above equation of KAW is simplified as [Streltsov et al., 1998]

$$(1 + \rho_i^2 k_x^2) \tilde{J}_{ix} = -i\omega \frac{\tilde{E}_x}{\mu_o V_A^2}. \quad (5)$$

The right-hand side is the polarization current due to the normal electric field  $E_x$ .  $-\rho_i^2 k_x^2 \tilde{J}_{ix}$  is the correction due to finite gyroradius.

Replacing  $ik_x$  with  $\partial_x$ , and  $-i\omega$  with  $\partial_t$ , we immediately find that equation (5) recovers most of equation (3). The  $E_y$  term in equation (3) is not recovered because  $E_y$  is not a component of KAW. Equation (3) describes the time-varying aspect of the Hall electric field, the normal component of the current density, and the reconnection electric field. Equation (5) describes the electric field and current of the KAW dynamics under the correction from the finite ion gyroradius effect. The similar format between equations (3) and (5) clearly indicates the following fact: the contribution to  $E_n$  from the ion pressure gradient represents the same finite ion gyroradius effect as that of KAW. The finite ion gyroradius effect of KAW is important in a finite plasma beta ( $> m_e / m_i$ ). The plasma beta is generally larger than 1 in the center of the reconnection layer. The beta is on the order of 0.1 at the edge of the reconnection layer in the magnetopause and magnetotail, indicating that the finite ion gyroradius effect is ubiquitously important for reconnection.

### 3. How Ion Intrusion May Produce the Perpendicular Electric Field in Reconnection

Equation (3) provides new insights into the nature of electric field and the ion motion in a reconnection layer. Ion intrusion corresponds to a certain profile of  $J_{ix}$ . From equation (3), we can infer what kind of ion intrusion ( $J_{ix}$ ) should produce a suitable electric field ( $E_x$  and  $E_y$ ) for reconnection to occur. Such a theoretical consideration is useful as the profile of ion intrusion may be predetermined by external condition or boundary conditions, for instance, at the magnetopause reconnection.

We illustrate how ion intrusion can produce  $E_x$  (and/or  $E_y$ ) in asymmetric reconnection as depicted in Figure 1b. In the asymmetric reconnection, magnetosheath ion enters the magnetosphere side due to ion gyroradius effect. For simplicity, we only consider the ion current from magnetosheath ions. The magnetosphere ion population is assumed at rest. The current from ion intrusion is toward the magnetosphere side. In this case, the term  $J_{ix}$  is negative. This term cannot support a positive  $E_y$  and a positive  $\partial_t E_x$  that are suitable for reconnection to occur. Only the gyroradius effect term  $-\rho_i^2 \nabla_{xx} J_{ix}$  can support a positive  $E_y$  and  $\partial_t E_x$  on the magnetosphere side. The term  $-\rho_i^2 \nabla_{xx} J_{ix}$  is the fluid manifestation of the finite ion gyroradius effect, leading to a nonlocal dependence of the perpendicular current on the electric field. As a result, the relative phase between  $J_{ix}$  and  $E_x$  can be complicated. Without losing generality, we set the boundary of magnetosheath ions at  $X = 0$ . Assuming that the penetration current of sheath ions decreases exponentially,  $J_{ix} = J_o e^{-|x|/\lambda}$  for  $X < 0$ , the left side of equation (3) becomes  $(1 - \rho_i^2 / \lambda^2) J_{ix}$ . To make the LHS positive, the penetration length  $\lambda$  has to be smaller than the ion gyroradius.

The above calculation provides the following perspective. Ion intrusions with a penetration length smaller than the ion gyroradius are more effective in triggering suitable electric fields (positive  $E_x$  and  $E_y$ ) for reconnection to occur.

#### 4. Hall Fields and Currents as Explained by KAW Eigenmode Theory

As previous sections show, KAW physics can explain the ion gyroradius effect resulting from ion pressure gradient. The normal electric field is clearly consistent with the electric field of KAW. If the electrons are frozen in at the ion scale, we still have  $\mathbf{E} + \mathbf{v}_i \times \mathbf{B} = (1/nq)\mathbf{J} \times \mathbf{B}$ . In this sense, the electric field of KAW may still be called a "Hall electric field." As shown in Figure 1, this normal electric field also corresponds to charge separation due to the intrusion of magnetosheath ion through finite gyroradius effect.  $J_{ix}$  and  $E_x$  have opposite signs during the generation of the KAW mode (Hall fields). According to the Poynting theorem, a negative  $\mathbf{J} \cdot \mathbf{E}$  contributes to the transfer of particle energy into the wave energy and thus the growth of the wave. Once the KAW mode is generated, it may be associated with energy dissipation [e.g., *Chaston et al., 2009, Liang et al., 2016*].

As ions move across magnetic field lines, electrons are dragged toward ions to try to keep neutrality. Mobile electrons stream along the magnetic field lines, forming the field-aligned currents. The total current  $\mathbf{J} = \mathbf{J}_i + \mathbf{J}_e$  needs to be divergence free to keep quasi-neutrality. As shown in Figure 1, the electron field-aligned currents produce the pattern of out-of-plane Hall magnetic fields. The field-aligned current and the associated out-of-plane  $B_m$  are parts of KAW. As KAWs are generated, the field-aligned currents propagate along the magnetic field line away from the reconnection site. The KAW propagation is characterized by a Poynting flux ( $E_n \times B_m$ ) that is mainly parallel/antiparallel the magnetic field line. The Hall fields propagate as KAWs structure along the magnetic field line away from the reconnection site. This important feature has been shown through explicit calculation [*Dai, 2009*] and demonstrated with particle-in-cell [*Shay et al., 2011*] and 3-D hybrid simulations [*Liang et al., 2016*].

As shown in Figure 1,  $E_n$  and  $B_m$  are mostly confined inside the current layer. This is due to the fact that KAW is in the form of eigenmode of the current layer. When the perpendicular scale of the waves is comparable to that of the inhomogeneity of the current layer, the WKB (Wentzel-Kramers-Brillouin) approximation for plane waves breaks down. A treatment of KAW eigenmode is necessary [*Lysak, 2008; Dai, 2009*].

KAW physics can predict the ratio ( $E_n/B_m$ ) of Hall fields. For KAW, the ratio  $E_n/B_m$  is  $V_A \sqrt{1 + k_x^2 \rho_i^2}$  [*Stasiewicz et al., 2000*]. In a reconnection current layer, this value should be on the order of 1 to several Alfvén speeds, because the perpendicular scale of the wave is the thickness of the reconnection layer and is comparable to ion gyroradius. The Alfvén speed varies significantly across the normal direction of the current layer. Calculations of discrete KAW eigenmode predict a  $E_n/B_m$  of 1 to a few Alfvén speeds based on the profile of the current layer [*Lysak, 2008; Dai, 2009*]. Notice that  $E_n$  and  $B_m$  are not in phase with each other in the wave source region. The Poynting flux of the generated KAW eigenmodes (Hall fields) can be directed either way in  $\pm \mathbf{Z}$  direction.

#### 5. Hall Fields and Currents: Whistler Mode, Tearing Mode, or KAW Mode?

In the original scenario proposed by *Sonnerup* [1979], quadrupolar out-of-plane Hall magnetic field  $B_m$  are considered as a static structure of the diffusion region. The Hall electric fields were absent in this original static picture. The presence of Hall electric field is important as it indicates a time-varying electromagnetic structure.

Terasawa [1983] described Hall fields as a current layer tearing eigenmode coupled with a shear Alfvén mode. In the coupled mode of Terasawa [1983], the out-of-plane Hall  $B_m$  (and  $V_m$ ) and field-aligned currents are actually components of the Alfvén mode. The tearing mode itself does not have the out-of-plane  $B_m$ . The Hall structure mostly consists of  $B_m$ ,  $E_m$ , and the in-plane Hall current. These components of field and current all belong to the Alfvén mode in the configuration of a reconnection layer. The polarization of the Hall structure is consistent with that of the Alfvén mode.

In theory, Hall fields have been linked to whistler mode [Mandt et al., 1994; Birn et al., 2001; Rogers et al., 2001] or KAW mode [Dai, 2009; Shay et al., 2011]. The quadrupolar out-of-plane Hall  $B_m$  has been explained in terms of either wave mode. To distinguish the mode of Hall fields, more comparisons between predictions and observations are needed. To this end, we emphasize two theoretical predictions that are unique nature of KAW.

1. As demonstrated in the previous sections, the balance of Hall electric fields by the ion pressure gradient represents the finite ion gyroradius effect of KAW. This effect depends on the ion temperature and is a key property that differentiates whistler from KAW.
2. Another prediction from KAW physics is the ratio of the Hall fields  $E_n/B_m$ .  $E_n/B_m$  should be on the order of the Alfvén speed if the Hall fields are of KAW in nature [Dai, 2009; Lysak, 2008].

These two predictions are unique nature of KAW mode, and their implications have not been fully recognized. In the following, we list the observational facts suggesting that Hall fields are well explained by predictions of KAW physics.

1. The normal electric field is mainly balanced by the ion pressure gradient [Burch et al., 2016b; Wang et al., 2016; Dai et al., 2015] (Y. Zhang et al., private communication, 2016). This is the manifestation of the finite ion gyroradius effect of KAW, as demonstrated in this study.
2. The ratio  $E_n/B_m$  is on the order of the Alfvén speed in many in situ observations (see more details in the appendix) [Mozer et al., 2002; Vaivads et al., 2004; Wygant et al., 2005; Eastwood et al., 2007; Phan et al., 2007; Retinò et al., 2007; Mozer et al., 2008; Dai et al., 2015; Duan et al., 2016; Burch and Phan, 2016]. This is a unique feature predicted by KAW physics.
3. In situ multipoint observations indicate that Hall fields are not static but slow-varying structures on timescale larger than the ion gyroperiod [Wygant et al., 2005; Vaivads et al., 2004]. The timescales of Hall field variations are consistent with KAW physics.
4. The polarization of Hall fields and Hall currents is consistent with KAW eigenmode of the current layer. The Hall fields are not consistent with tearing mode. In particular, the field-aligned current of the Hall current system is consistent with Alfvén mode and not consistent with low-frequency fast mode.
5. Hall fields and currents are observed at large distance from the reconnection site [Duan et al., 2016; Yamade et al., 2000; Fujimoto et al., 2001; Nakamura et al., 2004]. The associated Poynting flux is mainly along the magnetic field [Duan et al., 2016]. These observations are a characteristic signature of the Alfvén mode as demonstrated by Dai [2009], Shay et al. [2011], and Liang et al. [2016].
6. Octupolar out-of-plane  $B_m$  has been observed in simulations [von der Pahlen and Tsiklauri, 2014; , 2015]. The octupolar out-of-plane  $B_m$  can be explained by the prediction of the high  $n$  number KAW eigenmode [Dai, 2009]. A superposition of  $n = 1$  and  $n = 3$  mode can produce octupolar structures of the out-of-plane  $B_m$ .

## 6. Summary and Conclusions

Motivated by MMS observations, we present theoretical arguments suggesting that the balance of normal electric field  $E_n$  by the ion pressure gradient is a manifestation of kinetic Alfvén wave (KAW) physics. The ion pressure gradient represents the finite gyroradius effect of KAW. KAW mode of the reconnection layer can explain the Hall currents and Hall magnetic fields as well. The KAW physics predicts that the ratio  $E_n/B_m$  is on the order of Alfvén speed as observed. These predictions of Hall fields are unique to a KAW physics explanation. We list observational facts that match predictions of KAW physics, providing strong evidence that reconnection Hall fields and currents are of KAW mode in nature.

KAW physics further provides new perspectives on how ion intrusion may trigger the perpendicular electric fields suitable for reconnection. As suggested by calculations, “sharp” ion intrusions with a penetration length smaller than ion gyroradius are more effective in producing suitable electric fields for reconnection to occur.

**Table A1.** List of Past Observations of the Ratio  $E_n/B_m$  as Compared With the KAW Prediction (a Few Alfvén Speed)

Event	Event Time	$\Delta E_n$	$\Delta B_m$	$E_n/B_m$	Alfvén Speed
Polar [Mozer et al., 2002]	2001-4-1, 05:46:30 UT–05:47:30 UT	30 mV/m	45 nT	670 km/s	1,240 km/s
Cluster [Vaivads et al., 2004]	2002-2-20, 13:22:02 UT–13:22:08 UT	15 mV/m	20 nT	750 km/s	311 km/s
Cluster [Wygant et al., 2005]	2001-10-1, 09:46:46 UT–09:46:52 UT	60 mV/s	6 nT	10,000 km/s	1,400 km/s
Cluster [Wygant et al., 2005]	2001-10-1, 09:46:40 UT–09:47:10 UT	40 mV/m	7 nT	6,000 km/s	1,400 km/s
Cluster [Eastwood et al., 2007]	2001-8-22, 09:40:00 UT–09:46:00 UT	40 mV/m	15 nT	2,600 km/s	1,740 km/s
Cluster [Phan et al., 2007]	2003-1-14, 06:11:30 UT–06:12:30 UT	7 mV/m	25 nT	280 km/s	190 km/s
Cluster [Retino et al., 2008]	2002-3-27, 10:16:51 UT–10:16:53 UT	9 mV/m	10 nT	900 km/s	210 km/s
THEMIS [Mozer et al., 2008]	2007-7-20, 17:38:15 UT–17:39:15 UT	8 mV/m	18 nT	440 km/s	890 km/s
THEMIS [Mozer et al., 2008]	2007-7-20, 17:43:00 UT–17:44:00 UT	8 mV/m	10 nT	800 km/s	1,320 km/s
THEMIS [Dai et al., 2015]	2013-2-13, 23:24:30 UT–23:25:30 UT	10 mV/m	8 nT	1,250 km/s	1,160 km/s
MMS [Burch et al., 2016a]	2015-10-16, 13:07:00 UT–13:07:04 UT	10–20 mV/m	15 nT	670–1,330 km/s	280 km/s
MMS [Burch et al., 2016a]	2015-12-8, 11:20:42 UT–11:20:45 UT	30 mV/m	15 nT	2,000 km/s	510 km/s
MMS (Y. Zhang et al., pers. comm., 2016)	2015-12-13, 10:31:18 UT–10:31:28 UT	15 mV/m	10 nT	1,500 km/s	620 km/s

## Appendix A

The KAW physics uniquely predict a ratio of Hall fields ( $E_n/B_m$ ) on the order of Alfvén speed. In the manuscript, we list a number of observations of Hall fields that is consistent with this prediction. The details on the ratio ( $E_n/B_m$ ) in previous observations are listed in Table A1.  $\Delta E_n$  and  $\Delta B_m$  are the peak values of Hall fields during the observations. The Alfvén speed is computed at the out edge of the current layer.

### Acknowledgments

This work was supported by NNSFC grants 41574161 and 41231067 and in part by the Specialized Research Fund for State Key Laboratories of China.

### References

- Birn, J., et al. (2001), Geospace Environmental Modeling (GEM) magnetic reconnection challenge, *J. Geophys. Res.*, *106*, 3715–3720, doi:10.1029/1999JA900449.
- Burch, J. L., and T. D. Phan (2016), Magnetic reconnection at the dayside magnetopause: Advances with MMS, *Geophys. Res. Lett.*, *43*, 8327–8338, doi:10.1002/2016GL069787.
- Burch, J. L., T. E. Moore, R. B. Torbert, and B. L. Giles (2016a), Magnetospheric multiscale overview and science objectives, *Space Sci. Rev.*, *199*(1), 5–21, doi:10.1007/s11214-015-0164-9.
- Burch, J. L., et al. (2016b), Electron-scale measurements of magnetic reconnection in space, *Science*, *352*, AAF2939, doi:10.1126/science.aaf2939.
- Cai, H., D. Ding, and L. Lee (1994), Momentum transport near a magnetic X line in collisionless reconnection, *J. Geophys. Res.*, *99*(A1), 35–42.
- Cai, H. J., and L. C. Lee (1997), The generalized Ohm's law in collisionless magnetic reconnection, *Phys. Plasmas*, *4*, 509–520, doi:10.1063/1.872178.
- Cassak, P., and M. Shay (2007), Scaling of asymmetric magnetic reconnection: General theory and collisional simulations, *Phys. Plasmas*, *14*, 102114.
- Chaston, C. C., et al. (2005), Drift-Kinetic Alfvén waves observed near a reconnection X line in the Earth's magnetopause, *Phys. Rev. Lett.*, *95*, 065002, doi:10.1103/PhysRevLett.95.065002.
- Chaston, C. C., J. R. Johnson, M. Wilber, M. Acuna, M. L. Goldstein, and H. Reme (2009), Kinetic Alfvén wave turbulence and transport through a reconnection diffusion region, *Phys. Rev. Lett.*, *102*(1), 015,001.1–015,001.4, doi:10.1103/PhysRevLett.102.015001.
- Cheng, C., and J. R. Johnson (1999), A kinetic-fluid model, *J. Geophys. Res.*, *104*(A1), 413–427.
- Cheng, C. Z. (1991), A kinetic-magnetohydrodynamic model for low-frequency phenomena, *J. Geophys. Res.*, *96*(A12), 21,159–21,171, doi:10.1029/91JA01981.
- Dai, L. (2009), Collisionless magnetic reconnection via Alfvén eigenmodes, *Phys. Rev. Lett.*, *102*, 245003, doi:10.1103/PhysRevLett.102.245003.
- Dai, L., C. Wang, V. Angelopoulos, and K.-H. Glassmeier (2015), In situ evidence of breaking the ion frozen-in condition via the non-gyrotropic pressure effect in magnetic reconnection, *Ann. Geophys.*, *33*, 1147–1153, doi:10.5194/angeo-33-1147-2015.
- Duan, S., L. Dai, C. Wang, J. Liang, A. Lui, L. Chen, Z. He, Y. Zhang, and V. Angelopoulos (2016), Evidence of kinetic Alfvén eigenmode in the near-Earth magnetotail during substorm expansion phase, *J. Geophys. Res. Space Physics*, *121*, 4316–4330, doi:10.1002/2016JA022431.
- Eastwood, J., et al. (2007), Multi-point observations of the Hall electromagnetic field and secondary island formation during magnetic reconnection, *J. Geophys. Res.*, *112*, A06235, doi:10.1029/2006JA012158.
- Fujimoto, M., T. Nagai, N. Yokokawa, Y. Yamada, T. Mukai, Y. Saito, and S. Kokubun (2001), Tailward electrons at the lobe-plasma sheet interface detected upon dipolarizations, *J. Geophys. Res.*, *106*(A10), 21,255–21,262.
- Hasegawa, A., and L. Chen (1976), Kinetic processes in plasma heating by resonant mode conversion of Alfvén wave, *Phys. Fluids*, *19*(12), 1924–1934.
- Johnson, J. R., and C. Cheng (1997), Kinetic Alfvén waves and plasma transport at the magnetopause, *Geophys. Res. Lett.*, *24*(11), 1423–1426.
- Keiling, A. (2009), Alfvén waves and their roles in the dynamics of the Earth's magnetotail: A review, *Space Sci. Rev.*, *142*, 73–156, doi:10.1007/s11214-008-9463-8.
- Liang, J., Y. Lin, J. R. Johnson, X. Wang, and Z.-X. Wang (2016), Kinetic Alfvén waves in three-dimensional magnetic reconnection, *J. Geophys. Res. Space Physics*, *121*, 6526–6548, doi:10.1002/2016JA022505.
- Lin, Y., J. R. Johnson, and X. Wang (2012), Three-dimensional mode conversion associated with kinetic Alfvén waves, *Phys. Rev. Lett.*, *109*(12), 125003.

- Lysak, R. L. (2008), On the dispersion relation for the kinetic Alfvén wave in an inhomogeneous plasma, *Phys. Plasmas*, 15(6), 062901.
- Lysak, R. L., and W. Lotko (1996), On the kinetic dispersion relation for shear Alfvén waves, *J. Geophys. Res.*, 101, 5085–5094, doi:10.1029/95JA03712.
- Mandt, M. E., R. E. Denton, and J. F. Drake (1994), Transition to whistler mediated magnetic reconnection, *Geophys. Res. Lett.*, 21, 73–76, doi:10.1029/93GL03382.
- Mauk, B. H., et al. (2016), The Energetic Particle Detector (EPD) investigation and the Energetic Ion Spectrometer (EIS) for the Magnetospheric Multiscale (MMS) Mission, *Space Sci. Rev.*, 199(1), 471–514, doi:10.1007/s11214-014-0055-5.
- Mozer, F. S., S. D. Bale, and T. D. Phan (2002), Evidence of diffusion regions at a subsolar magnetopause crossing, *Phys. Rev. Lett.*, 89(1), 015002, doi:10.1103/PhysRevLett.89.015002.
- Mozer, F. S., V. Angelopoulos, J. Bonnell, K. H. Glassmeier, and J. P. McFadden (2008), THEMIS observations of modified Hall fields in asymmetric magnetic field reconnection, *Geophys. Res. Lett.*, 35, L17504, doi:10.1029/2007GL033033.
- Nakamura, R., et al. (2004), Flow shear near the boundary of the plasma sheet observed by Cluster and Geotail, *J. Geophys. Res.*, 109, A05204, doi:10.1029/2003JA010174.
- Phan, T., J. Drake, M. Shay, F. Mozer, and J. Eastwood (2007), Evidence for an elongated (>60 ion skin depths) electron diffusion region during fast magnetic reconnection, *Phys. Rev. Lett.*, 99(25), 255002, doi:10.1007/s11214-016-0245-4.
- Pollock, C., et al. (2016), Fast plasma investigation for magnetospheric multiscale, *Space Sci. Rev.*, 199(1), 331–406, doi:10.1007/s11214-016-0245-4.
- Retinò, A., D. Sundkvist, A. Vaivads, F. Mozer, M. André, and C. Owen (2007), In situ evidence of magnetic reconnection in turbulent plasma, *Nat. Phys.*, 3(4), 236–238.
- Rogers, B. N., R. E. Denton, J. F. Drake, and M. A. Shay (2001), Role of dispersive waves in collisionless magnetic reconnection, *Phys. Rev. Lett.*, 87, 195004, doi:10.1103/PhysRevLett.87.195004.
- Shay, M., J. Drake, J. Eastwood, and T. Phan (2011), Super-Alfvénic propagation of substorm reconnection signatures and poynting flux, *Phys. Rev. Lett.*, 107, 065001.
- Shay, M., T. Phan, C. Haggerty, M. Fujimoto, J. Drake, K. Malakit, P. Cassak, and M. Swisdak (2016), Kinetic signatures of the region surrounding the X line in asymmetric (magnetopause) reconnection, *Geophys. Res. Lett.*, 43, 4145–4154, doi:10.1002/2016GL069034.
- Sonnerup, B. U. Ö (1979), Magnetic field reconnection, in *Solar System Plasma Physics*, edited by L. J. Lanzerotti, C. F. Kennel, and E. N. Parker, pp. 45–108, North Holland, New York.
- Stasiewicz, K., et al. (2000), Small scale Alfvénic structure in the aurora, *Space Sci. Rev.*, 92, 423–533, doi:10.1007/BF02733547.
- Streltsov, A., W. Lotko, J. Johnson, and C. Cheng (1998), Small-scale, dispersive field line resonances in the hot magnetospheric plasma, *J. Geophys. Res.*, 103(A11), 26,559–26,572.
- Terasawa, T. (1983), Hall current effect on tearing mode instability, *Geophys. Res. Lett.*, 10, 475–478.
- Torbert, R. B., et al. (2016), The fields instrument suite on MMS: Scientific objectives, measurements, and data products, *Space Sci. Rev.*, 199(1), 105–135, doi:10.1007/s11214-014-0109-8.
- Vaivads, A., Y. Khotyaintsev, M. André, A. Retinò, S. C. Buchert, B. N. Rogers, P. Décréau, G. Paschmann, and T. D. Phan (2004), Structure of the magnetic reconnection diffusion region from four-spacecraft observations, *Phys. Rev. Lett.*, 93(10), 105001, doi:10.1103/PhysRevLett.93.105001.
- von der Pahlen, J. G., and D. Tsiklauri (2014), Octupolar out-of-plane magnetic field structure generation during collisionless magnetic reconnection in a stressed x-point collapse, *Phys. Plasmas*, 21(6), 060705.
- von der Pahlen, J. G., and D. Tsiklauri (2015), The effects of ion mass variation and domain size on octupolar out-of-plane magnetic field generation in collisionless magnetic reconnection, *Phys. Plasmas*, 22(3), 032905.
- Wang, S., et al. (2016), Two-scale ion meandering caused by the polarization electric field during asymmetric reconnection, *Geophys. Res. Lett.*, 43, 7831–7839, doi:10.1002/2016GL069842.
- Wu, D.-J., G.-L. Huang, D.-Y. Wang, and C.-G. Fälthammar (1996), Solitary kinetic Alfvén waves in the two-fluid model, *Phys. Plasmas*, 3(8), 2879–2884.
- Wygant, J. R., et al. (2005), Cluster observations of an intense normal component of the electric field at a thin reconnecting current sheet in the tail and its role in the shock-like acceleration of the ion fluid into the separatrix region, *J. Geophys. Res.*, 110, A09206, doi:10.1029/2004JA010708.
- Yamade, Y., M. Fujimoto, N. Yokokawa, and M. Nakamura (2000), Field-aligned currents generated in magnetotail reconnection: 3D Hall-MHD simulations, *Geophys. Res. Lett.*, 27(8), 1091–1094.